Int. J. Heat Mass Transfer. Vol. 27, No. 5, pp. 717-722, 1984
Printed in Great Britain

0017-9310/84 $3.00 + 0.00

THE NONDARCY REGIME FOR VERTICAL BOUNDARY LAYER NATURAL CONVECTION IN A POROUS MEDIUM

ADRIAN BEJAN and DIMOS POULIKAKOS
Department of Mechanical Engineering, Campus Box 427,
University of Colorado, Boulder, CO 80309, U.S.A.

(*Received* 26 *January* 1983 *and in revised form* 17 *August* 1983)

Abstract—This paper reports similarity solutions for vertical boundary layer natural convection near a solid wall adjacent to a fluid-saturated porous medium, in the case where the pore Reynolds number is high enough for the Darcy flow model to break down. Based on scaling arguments, it is shown that the departure from the Darcy flow model is dictated by the dimensionless number $G = (\nu/K)(bg\beta\Delta T)^{-1/2}$, with $G \to 0$ representing the high pore Reynolds number limit, and with $G \to \infty$ representing the Darcy flow limit. Similarity solutions are reported for flow and heat transfer in the following cases: (1) the nonDarcy limit $G = 0$ near an isothermal wall and near a constant-heat-flux wall, and (2) the intermediate regime $G = O(1)$ for natural convection near an isothermal wall. It is shown that the heat transfer results differ fundamentally from those known from traditional Darcy flow studies.

NOMENCLATURE

b	constant, equation (1)
B	function in Forschheimer's law, equation (2)
c_p	fluid specific heat at constant pressure
F	similarity function, equations (19) and (37)
g	gravitational acceleration
G	dimensionless group, equation (16)
H	vertical dimension
k	thermal conductivity of fluid/porous matrix combination
K	permeability
Nu_y	local Nusselt number, equations (24) and (36)
P	pressure
q	local velocity
q''	uniform wall heat flux
r	dimensionless parameter, equation (40)
Ra	Darcy-modified Rayleigh number, $g\beta HK\Delta T/\alpha\nu$
Ra_∞	large-Reynolds-number-limit Rayleigh number, $g\beta H^2\Delta T/b\alpha^2$
Ra_*	Darcy-modified Rayleigh number based on constant heat flux, $g\beta H^2Kq''/k\alpha\nu$
$Ra_{\infty *}$	large-Reynolds-number-limit Rayleigh number based on constant heat flux, $g\beta H^3q''/kb\alpha^2$
T	temperature
T_0	wall temperature
T_∞	fluid temperature far away from the wall
ΔT	temperature difference
u	horizontal velocity
v	vertical velocity
x	horizontal Cartesian coordinate
y	vertical Cartesian coordinate.

Greek symbols

α	thermal diffusivity, $k/(\rho c_p)$
β	coefficient of thermal expansion
δ	boundary layer thickness
η	similarity variable, equation (17b)
θ	dimensionless temperature
Θ	similarity function, equation (32)
μ	viscosity
ν	kinematic viscosity, μ/ρ
ρ	fluid density
ψ	streamfunction.

Subscripts

$*$	dimensionless quantity
1	pertaining to the uniform wall flux solution, equations (28)–(35).

INTRODUCTION

ONE OF the most basic problems in natural convection heat transfer is the buoyant boundary layer flow along a heated vertical wall adjacent to a fluid-saturated porous medium. This basic problem was analyzed for the first time by Cheng and Minkowycz [1] who relied on the theoretical framework provided by boundary layer theory. The same phenomenon has been studied in related configurations such as the flow on the outside of a vertical cylindrical surface imbedded in a porous medium [2], or the flow along the inner wall of a cylindrical well filled with porous material [3]. The time-dependent boundary layer flow triggered by the sudden imposition of a temperature difference between a wall and a fluid-saturated medium was studied just recently [4].

Among the practical considerations that stimulate the continuing interest in this flow is the engineering of efficient thermal insulation systems. This is why the vertical boundary layer concept has been used consistently in the analytical treatment of natural convection in an enclosed space filled with porous medium. The boundary layer treatment of enclosed porous layers began with Weber's paper [5] and continued with the works of Simpkins and Blythe [6, 7], Blythe *et al.* [8], Bejan [9] and Bergholz [10].

The objective of the present article is to relax a major assumption that limits the applicability of all the analytical results reported in the literature reviewed above. All these results are based on the Darcy flow model [11, 12], therefore, they are valid strictly in the limit where the Reynolds number based on volume-averaged velocity and pore length scale is less than $O(1)$. In addition to its relevance to slow-flow applications, one of the chief advantages of the Darcy flow model is that it linearizes the momentum equations, thus enabling the analyst to deal only with the nonlinearity of the energy equation. Theoretically, however, there is an important reason for relaxing the Darcy flow assumption from the analysis of vertical boundary layer convection. In any finite-size porous system, the boundary layer treatment of the flow is most appropriate in the Rayleigh number limit $Ra \rightarrow \infty$, which is precisely the limit where the Darcy flow model breaks down (because the vertical velocity scale increases as Ra). Throughout the Rayleigh number range one can envision, the Darcy flow model deteriorates as the boundary layer approximation improves, and vice versa. The analysis presented below resolves this conflict; its contribution is a boundary layer description valid for all values of pore Reynolds number.

MATHEMATICAL FORMULATION

The departure from Darcy's law in the limit of high pore Reynolds number is described by Forschheimer's modification [12, 13]

$$\nabla P - \rho \bar{g} = -\frac{\mu}{K} B(q)\bar{u}, \tag{1}$$

where

$$B = 1 + \frac{bK\rho}{\mu} q. \tag{2}$$

In the above equations $\bar{g}$ is the gravity vector, q the local speed and b an empirical constant of the porous medium (the units of b are m^{-1}). Eliminating the pressure term by taking the curl of equation (1) and invoking the Boussinesq approximation $\rho = \rho_0[1-\beta(T-T_0)]$ we obtain a single momentum equation which, relative to the vertical wall configuration sketched in Fig. 1, reads

$$\frac{\mu}{K}\left[\frac{\partial}{\partial x}\{B(q)v\} - \frac{\partial}{\partial y}\{B(q)u\}\right] = \rho_0 g \beta \frac{\partial T}{\partial x}. \tag{3}$$

The mathematical formulation is completed by writing the mass and energy conservation statements

$$\frac{\partial u}{\partial x} + \frac{\partial v}{\partial y} = 0, \tag{4}$$

$$u\frac{\partial T}{\partial x} + v\frac{\partial T}{\partial y} = \alpha\left(\frac{\partial^2 T}{\partial x^2} + \frac{\partial^2 T}{\partial y^2}\right). \tag{5}$$

We note at this point that equations (3)–(5) are based on the homogeneous porous medium model whereby α is the thermal diffusivity $k_{\text{medium}}/(\rho c_p)_{\text{fluid}}$ only.

Equations (3)–(5) are sufficient to reveal the proper length and velocity scales that rule the boundary layer region sketched with a dotted line on Fig. 1. Let δ be the unknown scale of the boundary layer thickness, and consider $\delta \ll H$; retaining only the largest terms, equations (3)–(5) dictate the following three equivalences of scales

$$\frac{u}{\delta} \sim \frac{v}{H}, \tag{6}$$

$$v\frac{\Delta T}{H} \sim \alpha \frac{\Delta T}{\delta^2}, \tag{7}$$

$$b\rho \frac{v^2}{\delta} \sim \rho g \beta \frac{\Delta T}{\delta}. \tag{8}$$

In writing equation (8) we made use of the fact that in the boundary layer limit [12, 13]

$$q = |v|(1+O(\delta/H)) \cong |v|, \tag{9}$$

and that $v > 0$ with respect to the coordinate system shown in Fig. 1. Solving equations (6)–(8) for the unknown scales u, v and δ yields

$$\delta \sim H\, Ra_\infty^{-1/4}, \quad v \sim \frac{\alpha}{H} Ra_\infty^{1/2}, \quad u \sim \frac{\alpha}{H} Ra_\infty^{1/4}. \tag{10}$$

The 'large-Reynolds-number-limit Rayleigh number' Ra_∞ is defined as

$$Ra_\infty = \frac{g\beta H^2 \Delta T}{b\alpha^2}. \tag{11}$$

This new number should not be confused with the traditional Darcy-modified Rayleigh number

$$Ra = \frac{g\beta H K \Delta T}{\alpha \nu},$$

used consistently in natural convection studies of the Darcy flow limit. The subscript '∞' chosen for Ra_∞ is intended to suggest that the new scaling (10) ultimately takes over as the traditional Ra becomes sufficiently high, i.e. as the Darcy flow model breaks down [how high Ra must become in order for scales (10) to apply is discussed later in connection with equation (16)].

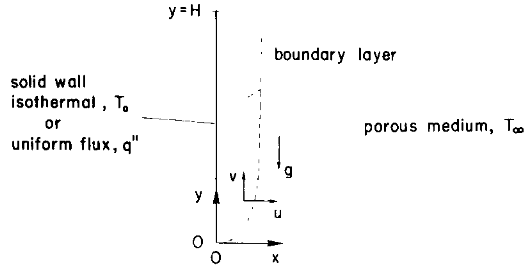

FIG. 1. Schematic of natural convection boundary layer flow near a vertical wall in a porous medium.

Scales (10) suggest the following dimensionless variables of $O(1)$

$$x_* = x/\delta, \quad y_* = y/H,$$
$$u_* = \frac{uH}{\alpha Ra_\infty^{1/4}}, \quad v_* = \frac{vH}{\alpha Ra_\infty^{1/2}}, \tag{12}$$
$$\theta = \frac{T-T_\infty}{T_0-T_\infty},$$

and, in terms of these, the dimensionless equations

$$\frac{\partial u_*}{\partial x_*} + \frac{\partial v_*}{\partial y_*} = 0, \tag{13}$$

$$u_* \frac{\partial \theta}{\partial x_*} + v_* \frac{\partial \theta}{\partial y_*} = \frac{\partial^2 \theta}{\partial x_*^2}, \tag{14}$$

$$G \frac{\partial v_*}{\partial x_*} + \frac{\partial v_*^2}{\partial x_*} = \frac{\partial \theta}{\partial x_*}. \tag{15}$$

The new dimensionless group

$$G = \frac{v}{K}(bg\beta\Delta T)^{-1/2}, \tag{16}$$

describes the extent to which the flow departs from the Darcy flow model. Thus, the focus of this study is on G values of $O(1)$ or less.

THE NONDARCY REGIME $G \to 0$

Constant wall temperature

Consider first the boundary layer driven by an isothermal vertical wall in a porous medium with (b, K) properties such that the G number may be regarded as zero in equation (15). Integrating equation (15) and invoking the outer condition $\theta = 0$ as $x \to \infty$ yields

$$v_* = \theta^{1/2}. \tag{17a}$$

Guided by the δ scale (10), we introduce the similarity variable

$$\eta = x_* y_*^{-1/2}. \tag{17b}$$

In this notation the dimensionless streamfunction ψ, defined as $u_* = \partial\psi/\partial y_*$ and $v_* = -\partial\psi/\partial x_*$, becomes

$$\psi = -y^{1/2}F(\eta), \tag{18}$$

where

$$F(\eta) = \int_0^\eta \theta^{1/2}\, d\eta. \tag{19}$$

We also have

$$u_* = -\tfrac{1}{2}y_*^{-1/2}(F-\eta F'), \tag{20}$$

and, from the boundary layer energy equation (14)

$$-\tfrac{1}{2}F\theta' = \theta''. \tag{21}$$

Noting that $v_* = \theta^{1/2} = F'$, equation (21) can be solved numerically based on a shooting technique subject to the following conditions

$$\theta(0) = 1, \quad F(0) = 0 \text{ and } \theta \to 0 \text{ as } \eta \to \infty. \tag{22}$$

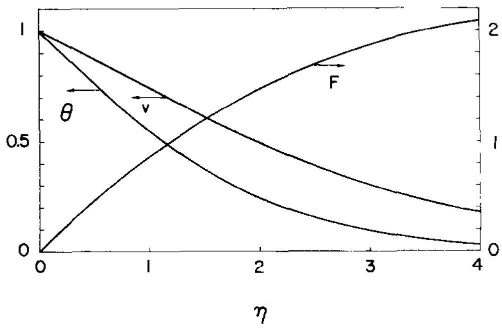

FIG. 2. Similarity solution for vertical velocity, temperature and streamfunction profiles in the nonDarcy limit ($G = 0$) near an isothermal wall.

These conditions represent, in order, the constant temperature and impermeability of the wall, and the constant temperature of the porous medium situated outside the boundary layer. The result of solving equation (21) numerically is shown in Fig. 2 as vertical velocity profile ($\theta^{1/2}$), temperature profile (θ) and streamfunction profile (F). These curves were obtained by marching in the positive η-direction in steps $\Delta\eta = 0.01$, which insured better than 1% accuracy in the heat transfer results presented in Table 1. The $\eta \to \infty$ condition (22) was satisfied at $\eta > 10$ by making the correct guess for the initial curvature of the temperature profile

$$\theta''(0) = -0.494. \tag{23}$$

From this result follows the local Nusselt number

$$Nu_y = \frac{q_y''}{\Delta T}\frac{y}{k} = 0.494(Ra_\infty)_y^{1/4}, \tag{24}$$

where the new Rayleigh number defined in equation (11) is now based on y as vertical length scale. The local Nusselt number (24) differs fundamentally from its counterpart in pure Darcy flow, $Nu_y = 0.444 Ra_y^{1/2}$ [1].

Uniform wall heat flux

The similarity solution for the case where q'' is constant and T_0 varies with altitude is pursued in a similar manner, by first noting the additional scaling law implied by writing $q'' = -k(\partial T/\partial x)_{x=0} = \text{const.}$, namely

$$\Delta T \sim \frac{q''\delta}{k}. \tag{25}$$

Table 1. Summary of numerical calculations for $Nu_y(Ra_\infty)_y^{-1/4} = -\theta''(0)$, or heat transfer in vertical boundary layer natural convection along an isothermal wall, when the flow deviates from the Darcy model

$G = \frac{v}{K}(bg\beta\Delta T)^{-1/2}$	$-\theta''(0) = \frac{Nu_y}{(Ra_\infty)_y^{1/4}}$
0	0.494
0.2	0.463
1	0.370
5	0.198

Combining this statement with scaling laws (6)–(8) derived previously from mass, energy and momentum considerations, yields the new scales

$$\delta \sim H\,Ra_{\infty *}^{-1/5}, \qquad v \sim \frac{\alpha}{H} Ra_{\infty *}^{2/5}, \qquad u \sim \frac{\alpha}{H} Ra_{\infty *}^{1/5}, \tag{26}$$

where $Ra_{\infty *}$ is the infinite-Reynolds-number-limit Rayleigh number based on constant heat flux

$$Ra_{\infty *} = \frac{g\beta H^3 q''}{k b \alpha^2}. \tag{27}$$

Defining a new set of dimensionless variables based on scales (26)

$$x_1 = \frac{x}{H} Ra_{\infty *}^{1/5}, \quad v_1 = \frac{vH}{\alpha} Ra_{\infty *}^{-2/5}, \quad u_1 = \frac{uH}{\alpha} Ra_{\infty *}^{-1/5}, \tag{28}$$

$$\theta_1 = \frac{T - T_\infty}{(q''/k) H\, Ra_{\infty *}^{-1/5}}, \tag{29}$$

the governing equations assume a form identical to equations (13)–(15) where G is taken as zero.

Similarity transformation is achieved by setting

$$\eta_1 = x_1 y_1^{-2/5}, \tag{30}$$

$$\psi_1 = -y_1^{3/5} F_1(\eta_1), \tag{31}$$

$$v_1^2 = \theta_1 = y_1^{2/5} \Theta(\eta_1), \tag{32}$$

where ψ_1 is defined in the usual manner, $u_1 = \partial\psi_1/\partial y_1$, $v_1 = -\partial\psi_1/\partial x_1$. Based on this transformation, the energy and momentum equations to be solved are

$$-\tfrac{3}{5} F_1 \Theta' + \tfrac{2}{5} F_1' \Theta = \Theta'', \tag{33}$$

$$F_1' = \Theta^{1/2}, \tag{34}$$

subject to the following conditions

$$\Theta'(0) = -1, \quad F_1(0) = 0, \text{ and } \Theta \to 0 \text{ as } \eta_1 \to \infty. \tag{35}$$

Equations (33) and (34) were integrated numerically yielding the velocity temperature and streamfunction profiles plotted in Fig. 3. The last of conditions (35) is satisfied if the integration is started with the guess that $\Theta(0) = 1.243$.

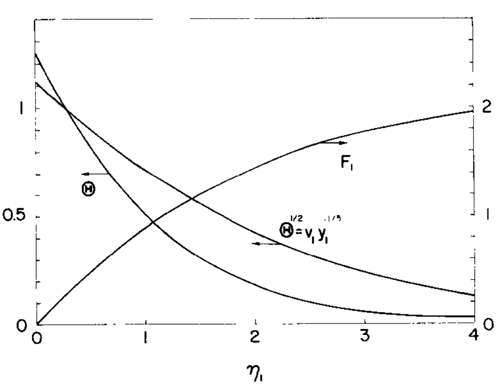

FIG. 3. Similarity solution for vertical velocity, temperature and streamfunction profiles in the nonDarcy limit ($G = 0$) near a constant-heat-flux wall.

The local Nusselt number along a constant-heat-flux wall is a way to calculate the actual wall–medium temperature difference: the similarity solution outlined above yields

$$Nu_y = \frac{q''}{T_0(y) - T_\infty} \frac{y}{k} = 0.804 (Ra_{\infty *})_y^{1/5}. \tag{36}$$

This heat transfer result differs markedly from its correspondent in the Darcy flow limit, $Nu_y = 0.772 (Ra_*)_y^{1/3}$, where Ra_* is the Darcy-modified Rayleigh number based on constant heat flux, $(Ra_*)_y = Kg\beta y^2 q''/(k\alpha\nu)$ [1].

THE INTERMEDIATE REGIME, $G = O(1)$

The gradual departure of the flow from the nonDarcy limit can be illustrated by considering the case of arbitrary G number in conjunction with the constant wall temperature boundary condition. In this case a similarity solution is possible because the boundary layer thickness varies as $H^{1/2}$ both in the nonDarcy limit, equations (10), and in the Darcy flow limit [1,5]. A similarity solution is not possible for the q'' = constant case, because δ increases as $H^{2/5}$ in the nonDarcy limit, equation (26), while in the Darcy flow limit it varies as $H^{1/3}$ [1].

The finite-G similarity solution is a generalization of the $G = 0$ solution presented early in the preceding section and in Fig. 2. The nondimensional formulation of the problem is already given in equations (13)–(15), and the similarity variables in equations (17) and (18). The only changes occur in the definition of stream-function profile, where

$$F = \frac{1}{2}\int_0^\eta [\sqrt{(4\theta + G^2)} - G]\, d\eta, \tag{37}$$

replaces equation (19), and in the momentum equation which now reads

$$(F')^2 + GF' = \theta. \tag{38}$$

Equations (38) and (21) were integrated numerically subject to conditions (22), using the shooting method described previously. Figures 4(a) and (b) show the evolution of the vertical velocity and temperature profiles as the G number increases, i.e. as the boundary layer approaches the traditional Darcy regime. Note that Figs. 4(a) and (b) are based on the $G = 0$ scaling described by equations (10); consequently, the vertical velocity scale and the boundary layer thickness are no longer $O(1)$ if the G number exceeds $O(1)$.

The heat transfer results obtained for finite G's are summarized in Table 1 and Fig. 5. The coefficient in the $Nu_y \sim (Ra_\infty)_y^{1/4}$ relation decreases steadily as G increases and as the flow plunges into the Darcy regime. In the present notation, the Darcy asymptote ($G \to \infty$) of ref. [1] is written as

$$Nu_y = 0.444 G^{-1/2} (Ra_\infty)_y^{1/4}, \tag{39}$$

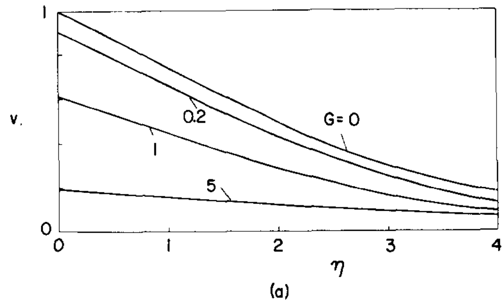

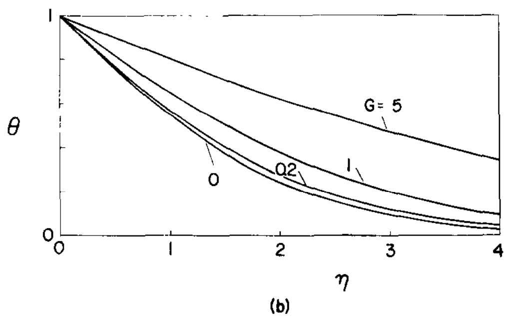

FIG. 4. The intermediate regime $G = O(1)$ near an isothermal wall: (a) vertical velocity profiles; (b) temperature profiles.

which accounts for the asymptotic behavior of $Nu_y/(Ra_\infty)_y^{1/4}$ on Fig. 5. Note that the finite-G heat transfer results generated by the similarity solution follow closely the Nusselt number curve derived based on the integral Kàrmàn–Pohlhausen method. The integral solution was derived in the usual manner [14], in this case assuming 'exponential-decay' velocity and temperature profile shapes as suggested by the Oseen-linearized solution to the boundary layer problem [5]. The integral solution yields

$$\frac{Nu_y}{(Ra_\infty)_y^{1/4}} = \left[\frac{r(4-r^2)}{12G}\right]^{1/2}, \qquad (40)$$

where

$$r = \frac{G^2}{2}\left[\left(1+\frac{4}{G^2}\right)^{1/2} - 1\right].$$

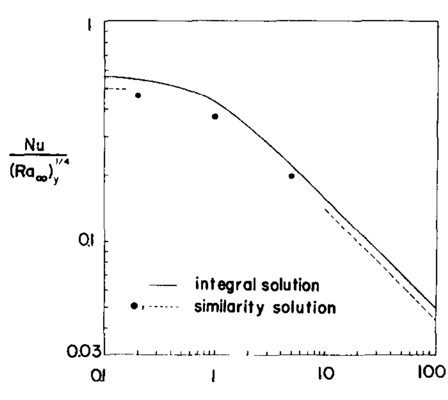

FIG. 5. Similarity and integral heat transfer results for the intermediate regime near an isothermal wall.

In the two G limits plotted on Fig. 5, $G \to 0$ and $G \to \infty$, the RHS of equation (40) yields $3^{-1/2}$ and $0.5G^{-1/2}$, respectively. These limits fall within 16% of the similarity solution asymptotes, 0.494 and $0.444G^{-1/2}$, respectively.

SUMMARY

In this article we reported the boundary layer solution to the problem of heat transfer along a vertical wall facing a porous medium, in the general case when the pore Reynolds number is not necessarily less than $O(1)$. We found that in the nonDarcy flow regime, or in the infinite pore Reynolds number limit, the boundary layer phenomenon is characterized by scales that differ markedly from the scales known in the Darcy limit. The new scales are given by equations (10) for an isothermal wall, and by equation (26) for a constant-heat-flux wall. The important dimensionless group for the non-Darcy regime is the new Rayleigh number Ra_∞ defined in equation (11) for an isothermal wall, and the corresponding group $Ra_{\infty *}$ defined by equation (27) for a constant-heat-flux wall.

The relative position of the boundary layer flow between the traditional Darcy limit [1] and the non-Darcy limit exhibited in Figs. 2 and 3 is described by the new dimensionless group G defined in equation (16). The intermediate flow regime characterized by G values of $O(1)$ was documented via the similarity solution presented in Figs. 4(a) and (b). The corresponding heat transfer rate was plotted in Fig. 5 next to the integral solution for the isothermal wall case. In the nonDarcy flow limit $G \to 0$ the local Nusselt number scales as $(Ra_\infty)_y^{1/4}$.

The contribution of the present study is measured graphically in Fig. 5: prior to this study, the only known results were the ones corresponding to the $G \to \infty$ limit (the Darcy flow limit). As argued in the Introduction, it is important to know the heat transfer picture in the entire G range because the Darcy model eventually breaks down as the boundary layer flow becomes more distinct (as Ra increases). As one anonymous reviewer pointed out, the need to modify the Darcy flow model was also discussed in ref. [15].

Acknowledgement—This work was supported in part by NSF Grant No. MEA-82-07779.

REFERENCES

1. P. Cheng and W. J. Minkowycz, Free convection about a vertical flat plate embedded in a saturated porous medium with application to heat transfer from a dike, *J. Geophys. Res.* **82**, 2040–2044 (1977).
2. W. J. Minkowycz and P. Cheng, Free convection about a vertical cylinder embedded in a porous medium, *Int. J. Heat Mass Transfer* **19**, 805–813 (1976).
3. A. Bejan, Natural convection in a vertical cylindrical well filled with porous medium, *Int. J. Heat Mass Transfer* **23**, 726–729 (1980).

4. D. B. Ingham, J. H. Merkin and I. Pop, Flow past a suddenly cooled vertical flat surface in a saturated porous medium, *Int. J. Heat Mass Transfer* **25**, 1916–1919 (1982).
5. J. W. Weber, The boundary layer regime for convection in a vertical porous layer, *Int. J. Heat Mass Transfer* **18**, 569–573 (1975).
6. P. G. Simpkins and P. A. Blythe, Convection in a porous layer, *Int. J. Heat Mass Transfer* **23**, 881–887 (1980).
7. P. A. Blythe and P. G. Simpkins, Convection in a porous layer for a temperature dependent viscosity, *Int. J. Heat Mass Transfer* **24**, 497–506 (1981).
8. P. A. Blythe, P. G. Daniels and P. G. Simpkins, Thermally driven cavity flows in porous media. I. The vertical boundary layer structure near the corners, *Proc. R. Soc. London* **A380**, 119–136 (1982).
9. A. Bejan, On the boundary layer regime in a vertical enclosure filled with a porous medium, *Lett. Heat Mass Transfer* **6**, 93–102 (1979).
10. R. F. Bergholz, Natural convection of heat generating fluid in a closed cavity, *J. Heat Transfer* **102**, 242–247 (1980).
11. J. Bear, *Dynamics of Fluids in Porous Media*, Chap. 5. Elsevier, New York (1972).
12. P. Cheng, Heat transfer in geothermal systems, *Adv. Heat Transfer* **14**, 1–105 (1979).
13. P. H. Forschheimer, *Z. Ver. Dt. Ing.* **45**, 1782–1788 (1901).
14. W. M. Rohsenow and H. Y. Choi, *Heat, Mass and Momentum Transfer*, pp. 160–162. Prentice-Hall, Englewood Cliffs, New Jersey (1961).
15. G. H. Evans and O. A. Plumb, 2nd AIAA/ASME Thermophys. and Heat Transfer Conf., Paper No. 78-HT-55 (1978).

LE REGIME NON DARCY POUR LA CONVECTION NATURELLE VERTICALE DE COUCHE LIMITE DANS UN MILIEU POREUX

Résumé—Ce texte concerne les solutions affines de convection naturelle de couche limite verticale près d'une paroi solide adjacente à un milieu poreux saturé en fluide, dans le cas où le nombre de Reynolds de pore est suffisamment grand pour que le régime de Darcy disparaisse. A patir d'arguments d'échelle, on montre que l'écart au modèle d'écoulement de Darcy est dicté par le nombre adimensionnel $G = (\nu/K)(bg\beta\Delta T)^{-1/2}$, avec $G \to 0$ représentant le limite de grand nombre de Reynolds de pore, et avec $G \to \infty$ représentant la limite de l'écoulement de Darcy. Des solutions affines sont données pour l'écoulement et le transfert thermique dans les cas suivants : (1) la limite $G = 0$ près d'une paroi isotherme et près d'une paroi à flux uniforme, et (2) le régime intermédiaire $G = O(1)$ pour la convection naturelle près d'une paroi isotherme. On montre que les résultats sur le transfert thermique diffèrent fondamentalement de ceux connus pour les études classiques de l'écoulement de Darcy.

DER NICHT-DARCYSCHE BEREICH FÜR DIE SENKRECHTE GRENZSCHICHTSTRÖMUNG IN EINEM PORÖSEN MEDIUM

Zusammenfassung—Für die freie Konvektion in der Grenzschicht einer festen Wand, welche aus porösem, fluidgesättigten Material besteht, werden Ähnlichkeitslösungen angegeben, und zwar für den Fall, daß die Poren-Reynolds-Zahl ausreichend groß ist, um das Darcy-Strömungsmodell zusammenbrechen zu lassen. Aufgrund von Ähnlichkeitsbetrachtungen zeigt sich, daß das Abrücken vom Darcy-Strömungsmodell von der dimensionslosen Zahl $G = (\nu/K)(bg\beta\Delta T)^{-1/2}$ gesteuert wird. $G \to 0$ entspricht der Begrenzung, durch die zu große Poren-Reynolds-Zahl, $G \to \infty$ der Darcy-Strömungsgrenze. Für Strömung und Wärmeübergang werden in folgenden Fällen Ähnlichkeitslösungen angeboten : (1) die nicht-darcysche Grenze $G = 0$ an einer isothermen Wand und an einer Wand mit konstanter Wärmestromdichte und (2) das mittlere Gebiet $G = O(1)$ für freie Konvektion an einer isothermen Wand. Dabei zeigt sich, daß Ergebnisse bezüglich des Wärmeübergangs grundlegend von denen abweichen, die von herkömmlichen Darcy-Strömungsuntersuchungen bekannt sind.

ЕСТЕСТВЕННАЯ КОНВЕКЦИЯ В ВЕРТИКАЛЬНОМ ПОГРАНИЧНОМ СЛОЕ В ПОРИСТОЙ СРЕДЕ ПРИ ОТКЛОНЕНИИ ОТ ЗАКОНА ДАРСИ

Аннотация—Представлены автомодельные решения для естественной конвекции в вертикальном пограничном слое у твердой стенки, прилегающей к насыщенной жидкостью пористой среде, в случае, когда число Рейнольдса для пор достаточно велико и модель Дарси для потока становится неприемлемой. Из соображений размерности показано, что отличие от модели Дарси определяется безразмерным числом $G = (\nu/K)(bg\beta\Delta T)^{-1/2}$, где $G \to 0$ соответствует верхнему пределу числа Рейнольдса для пор, а $G \to \infty$ — пределу потока Дарси. Даны автомодельные решения для массо- и теплопереноса в случае (1) предела $G = 0$ (наибольшее отклонение от закона Дарси) для изотермической стенки и стенки с постоянной плотностью теплового потока и (2) промежуточного режима $G = O(1)$ для естественной конвекции у изотермической стенки. Показано, что данные по теплопереносу значительно отличаются от результатов, полученных в традиционных исследованиях потоков, подчиняющихся закону Дарси.